

Quantum Listenings

Amateur Sonification of Vacuum and other Noises

Carsten Henkel^{1,*}

¹Universität Potsdam, Institut für Physik und Astronomie, Germany

Abstract. The sensory perceptions of vision and sound may be considered as complementary doorways towards interpreting and understanding physical phenomena. We provide a few selected samples where scientific data of systems usually not directly accessible to humans may be listened to. The examples are chosen close to the regime where quantum mechanics is applicable. Visual and auditory renderings are compared with some connections to music, illustrating in particular a kind of fractal complexity along the time axis.

1 Introduction

“Do you see this point? – No, I do not understand.” This fictitious sample of a dispute points to the conceptual links between sensory perception (seeing, hearing) and logical or physical explanations which may be the key achievements of the natural sciences. In this paper, I would like to discuss the complementarity in illustrating physical phenomena with two-dimensional graphics and acoustic signals, with the aim of comparing ways of understanding. A picture may be captured at a glance, while listening to a sentence develops in time. In particular perceiving and memorizing sound seems to proceed in a fractal way as time unfolds. This is in part due to the physical processes of sound generation like the many attributes of a tone in musical acoustics (spectral color, pitch, attack, fading ...). On the other hand, the brain seems to function by compressing acoustic information in a formidable way, building on recognizable “molecular unit” patterns and then organising them in a hierarchical way from phrases to epochs in the history of music.

In this paper, we review a few basic properties of perceiving and encoding sound (Sec. 2.1). We then give examples for mapping observables from the atomic or molecular scale to sound (Secs. 2.3, 2.4). In Secs. 3.2, 3.3, spectra of quantum noise are discussed and converted into the audio range. Next to the examples, we a few exercises are suggested for further applications.

This material is provided by an amateur of sonification and is by no means meant to be comprehensive. Useful resources can be found via the conference series on auditory display and its web site [1]. The chosen examples hopefully help to appreciate the many facets of complexity and disorder in the physical world. Audio files are available from the repository gitup.uni-potsdam.de/henkel/sonification_cd25 [2]; supplementary material is provided in the preprint [3].

*e-mail: carsten.henkel@uni-potsdam.de

2 Basics of Sonification

2.1 Human sound perception

The sensorial apparatus for auditory perception of a young person spans the frequency range of 20 Hz–20 kHz. This is about 2^{10} , i.e., ten octaves, much wider than the single octave of the visible spectrum (between $c/780$ nm and $c/380$ nm). Frequencies below 10 Hz are perceived in the time domain via the onset and fading of a sound. This illustrates an interesting “separation of time scales” that provides the basis for mapping one-dimensional sound data into a two-dimensional time-frequency representation (see Sec. 3.1). The inner ear is performing a spectral analysis over the mentioned frequency range on times scales faster than 100 msec, as listeners trained to musical samples may testify.

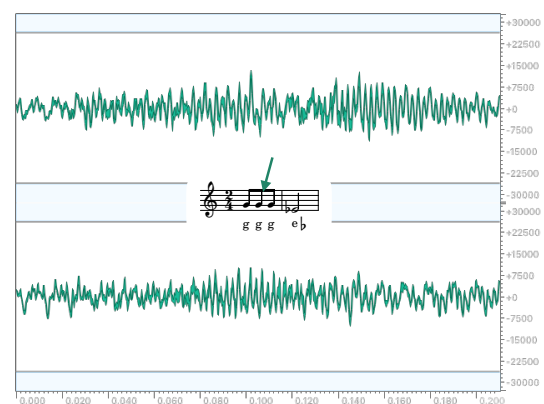


Figure 1. Example of an acoustic waveform (two stereo channels are shown). These 210 ms represent the 2nd eighth note (see insert, $g^1 \approx 392$ Hz, i.e. period 2.55 ms) of Beethoven’s 5th Symphony, 1st Movement (c minor, op. 67) [4]. Audio file: [Beethoven5_2nd-8th.mp3](#).

Modern sound treatment is done in a discrete (digital) representation where an acoustic signal is a sequence $u(t_i)$ of integers in the range $-2^{15} \leq u < 2^{15} = 32\,768$ (16 bit depth amplitude) and the elementary time step is $dt = 1/44.1\text{ kHz} = 22.7\ \mu\text{s}$. The physical properties of the signal are often quantified using logarithmic scales, for example the familiar decibel (dB) unit for loudness. Since you may easily turn down the volume, we focus here on typical scales in the time and frequency domains. An example is provided in Fig. 1 where the stereo channels over a duration of 200 msec for a single note are shown. The eye barely makes sense of these erratic signals, but try to listen to this sample (see caption). Although it covers less than 100 periods of the fundamental vibration (and less than 10^4 data points per channel), we seem to recognise that this was played by a string orchestra (!).

2.2 Mapping to sound

To illustrate frequencies, the piano keyboard or musical notation in general is a perhaps familiar example. Tones in music are organised in a logarithmic scale, each factor of two being represented by a fixed distance (one octave). A linear progression of frequencies, naturally provided by the harmonics of a periodic signal, thus clusters into narrower intervals in the musical sense, as the number of harmonics grows beyond eight (Fig. 2). The seventh harmonic already falls between the discrete notes used in western music, and a quarter tone only provides an approximation. As musical notes increase in pitch, their absolute frequency spacing hence increases, which is not much different from the distribution of prime numbers (first studied by Gauß and Legendre).



Figure 2. Harmonics of D ($\approx 73\text{ Hz}$) up to the eighth (three octaves). In the usual tuning, the 6th harmonic appears at $a^1 = 440\text{ Hz}$. The 7th harmonic appears approximately a quarter tone below $c^2 = 523\text{ Hz}$, i.e., at $\approx 508\text{ Hz}$ (accidental \sharp), cf. audio file [obertonreihe.mp3](#). (In diatonic tuning, D would appear at $440/6 = 73.333\text{ Hz}$, in well-tempered tuning, at $2^{-7/12} 440/4 = 73.416\text{ Hz}$.)

The fundamental musical identification of tones separated by an octave introduces a periodicity along the (logarithmic) frequency axis. The lettering of notes in music is a prime example. Variants of this “coding” can be used for “mathematical compositions” in the spirit of Iannis Xenakis [5]. One brief illustration is provided in Fig. 3 (see also Figs. 11–13 in the Supplementary Material [3]). In homage to J. S. Bach and A. Schönberg, the well-tempered chromatic scale with its twelve evenly spaced notes (ratio $2^{1/12}$), is used to represent the digits $0, 1 \dots 9, 10 = a, 11 = b$ in base 12. Taking the digits

π as a never-ending resource, one gets the upper voice of the score in Fig. 3. The lower voice is computed from Euler’s number e , but represented in base 5. Its are converted into another musical set of notes, the pentatonic scale. We take the same subset as the incipit of M. Mussorgsky’s “Promenade” from *Pictures of an Exhibition*. The audio file [pi_over_e_classical.mp3](#) and other variations can be downloaded from the repository mentioned in the Introduction [2]. In the “ π/e walk” (Fig. 12 of Ref. [3]), the music is allowed to wander up and down beyond a single octave, similar to Brownian motion.



Figure 3. Sonified duet of π over e . The digits of π in base twelve are encoded into the well-tempered half-tones from f^1 to e^2 , while e ’s digits in base five are mapped to a pentatonic scale. The only manual edits were applied to duration: the first note and the digit 0 getting longer durations. For a longer version, see Fig. 11 in Ref. [3] and audio file [pi_over_e_classical.mp3](#).

Such a piece may be perceived *prima vista* as “complex”, and when listening, it sounds “disordered” or even “pointless”. Ear and brain, at least when building on classical western music education, are missing “structures”. These are expected to be fractal in time, grouping tones into basic motifs, phrases, themes, and entire movements. This melody, however, seems to crumble and decompose into its atoms. Each of the notes is highly conventional (at least in the violin/bassoon chosen instrumentation), but taken as a sequence, they do not blend easily into larger musical structures. It does not come as a surprise that any “interesting” sequence of numbers can be found in the digits of an irrational number like π or e . And indeed, after a few listenings, also the ear starts to remember (recognize) certain fragments, and be they the somehow artificially longer notes of the 0 digit. An example for an extended fragment that somehow “makes (musical) sense” is highlighted in Fig. 11 of Ref. [3] (grey bars), corresponding to the digits 1332 34411 23230 in the lower voice. This impression quite probably arises because the second group nearly repeats the first one, bringing forward a connection between “sense” and “lower entropy”. Indeed, both concepts fundamentally relate to the compression of data, as illustrated by constructing entropy from Shannon’s information theory concepts.

2.3 A simple quantum chord

More abstract examples of sound can be constructed based on the physics of vibrations like in electrodynamics and quantum mechanics. Nearly hundred years ago, when the first Raman spectra were recorded, Andrews mapped the lines found for substances like ethanol or gasoline into a set of music notes, as described in Ref. [7]. Indeed Quoting one of the quantum founders, A. Sommerfeld [6]:

“[Die Quantentheorie] ist das geheimnisvolle Organon, auf dem die Natur die Spektralmusik spielt und nach dessen Rhythmus sie den Bau der Atome und Kerne regelt.” – Quantum theory is the mysterious organ which Nature is playing its spectral music on and whose rhythm She uses to build and rule atoms and nuclei. (Transl. C.H.)

This idea has blossomed in recent years to produce the field of quantum sonification. A few entry points into it can be found in Refs. [8–10]. If we turn to the simplest quantum system with a discrete spectrum, this is probably the Hydrogen atom. Indeed, the energy levels of the harmonic oscillator have already been illustrated by the harmonics of Fig. 2. There are infinitely many bound levels in Hydrogen and other atoms due to the long-range Coulomb interaction. The usual representation is putting the ground state at the bottom, less strongly bound levels appear above it. In terms of frequencies, the reverse ordering may be more natural. We thus take the binding energies $E_n = 1/2n^2$ a.u. of the Balmer formula and translate them into a frequency in the acoustic range. Restricting ourselves for simplicity to the 88 keys on the piano, we are limited to a ratio from highest to lowest frequencies of $2^{87/12} \approx 150$. We map the $n = 1$ level (binding energy 13.6 eV) to a very high key ($a^4 = 3520$ Hz) and find that the lowest one that would still be playable on the piano is the Rydberg level $n = 11$ (0.112 eV, see the key $B_2^b \approx 29$ Hz in Fig. 4). An unusual aspect of this representation is the relatively wide spacing between large- n levels, which arises, of course, from the logarithmic map to the musical keyboard. – As an intriguing **exercise**, look up a few low-lying levels of the alkali atoms, say, and play the corresponding quantum (defect) chords.

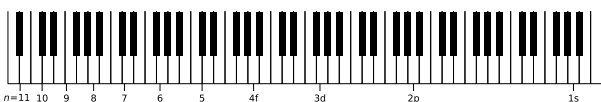


Figure 4. Frequencies corresponding to the binding energies of the Hydrogen atom mapped to a piano keyboard. Note the beautiful features of “atomic harmony” [6]: the levels $n = 2, 3$ are separated by two fifths (ratio $(2/3)^2$) and 3, 4 by two fourths $((3/4)^2)$. (The slight offset of the levels $n = 3, 6$ with respect to the keys is actually due to the well-tempered tuning assumed here where fifths and fourths are not “pure”.) The audio file [hydrogen_keys.mp3](#) renders the frequencies approximately on a well-tempered keyboard, including quarter tones.

How would the time scales due to the lifetimes of atomic levels translate into this acoustic picture? We may represent a decaying state as a pure tone with a slowly decreasing intensity. After exciting the atom with a laser pulse to the Rydberg level $10p_{3/2}$, say, a deep vibration (the lowest $C\sharp_1$ key, 34.7 Hz, in Fig. 4) would signal the occupation of this state. Its radiative decay is, however, very long compared to the electronic oscillation period (binding frequency 32.9 THz measured relative to the ion-

ization potential) [11]. The fastest decay channel is to the 1s state with an Einstein coefficient $A = 4.21E06/s$, and in the “keyboard representation”, its actual decay time would be more than two days (!). Even the Lyman- α line ($2p \rightarrow 1s$, 122 nm) which has a much shorter lifetime ($A = 6.265E08/s$) would have 2p “vibrate” for more than an hour.

An interesting question is whether the ear is able to perceive phase relations between harmonics. For quantum states, this is equivalent to telling apart a coherent superposition from a statistical mixture. Conversely, stereo audio signals can be used to bring coherences to sound, thanks to binaural hearing [9]. In any case, to provide an actual ensemble, one would have to resort to ergodicity and perform a statistical analysis over some time window. We come back to the corresponding autocorrelation functions in Sec. 3.1.

2.4 Molecular vibrations

Scanning microscopes are powerful instruments to image the world of atoms and molecules. In these devices, a sharp tip is mounted on a flexible beam (cantilever) and is approached to a solid sample using piezo-control stages. The cantilever can be modelled as a weakly damped harmonic oscillator which is subject to a force with a steep distance dependence:

$$m(\ddot{z} + \gamma\dot{z} + \Omega^2(z - z_0)) = -\frac{\partial V}{\partial z} + f(t), \quad (1)$$

where m is an effective mass, z_0 the nominal equilibrium position, and $f(t)$ an external drive. A typical interaction potential is of the Lennard-Jones type

$$V(z) = -\frac{c_3}{3z^3} + \frac{c_9}{9z^9}. \quad (2)$$

At large distance, expanding the potential around the equilibrium position z_0 , one gets a complex dispersion relation

$$\omega^2 + i\gamma\omega - \Omega^2 + \frac{4c_3}{mz_0^5} - \frac{10c_9}{mz_0^{11}} = 0. \quad (3)$$

Neglecting the last term, the long-range surface attraction downshifts by its intrinsic curvature (second derivative) the cantilever vibration. This is a common method to measure surface forces [12], but requires some model assumptions to reconstruct a full force-distance curve. As the cantilever approaches the surface, the linearization behind Eq. (3) breaks down, and the vibration becomes anharmonic. This is shown in Fig. 5 where the numerical solution to Eq. (1) is plotted: the upper left panels give the quadratures in the time domain, the lower right ones the spectrum of the vibration. Upon approaching a sample, eventually neither the natural spring constant $k = m\Omega^2$ nor the piezo-control force are able to compensate for the attractive forces: the cantilever then moves into a second equilibrium position closer to the surface. Right at the transition, the potential is bistable [around distance 0.60 nm in Fig. 5(c)]. Between this point and 0.57 nm,

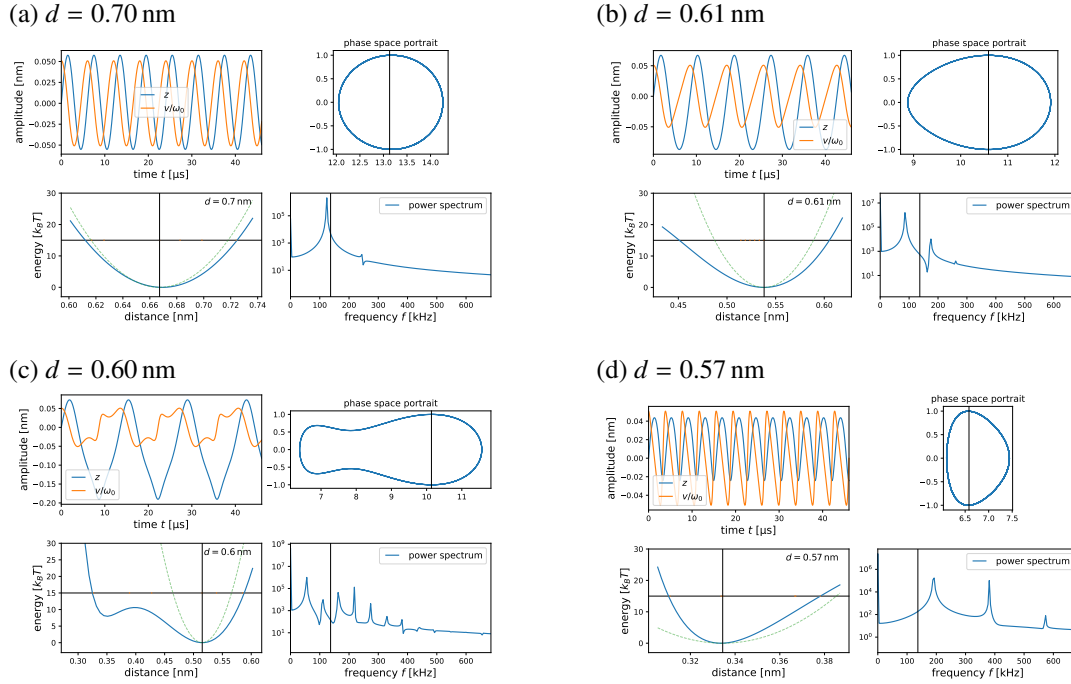


Figure 5. Analysis of nonlinear oscillations upon approaching a cantilever to a solid surface. In each of the four panels, one finds at top left: trajectory, top right: phase space portrait, bottom left: effective potential including a harmonic contribution from the piezo-control, bottom right: power spectrum (Fourier transform) of the vibration. The oscillation occurs at a fixed energy about $15 k_B T$ above the potential minimum (horizontal line). The vertical line in the spectra marks the eigenfrequency $\Omega/2\pi \approx 140$ kHz. In the acoustic version ([listen_approach_curve.mp3](#)), the time series has been re-scaled to that $\Omega/2\pi$ corresponds to roughly 400 Hz.

the down-shifted vibration disappears and is replaced by a strongly coloured spectrum with many harmonics.

It is quite interesting to appreciate these features acoustically from the provided .mp3 file. The sonification is generated from the numerical solution with the `scipy.io.wavfile` package. The nominal frequency $\Omega/2\pi$ has been mapped to the audio band. We have used audio software to remove phase jumps that slipped into the simulated raw data and to patch datasets at different distances into a single file. It is surprising that in acoustic synthesis of this kind, the ear clearly perceives a single phase slip or discontinuity as a “knack”. Actual experimental data also contain a noise floor due to amplifiers and the intrinsic thermal motion, as can be heard in Ref. [10]. A natural **exercise** to take this into account would be a stochastic model with an additional Langevin force on the rhs of Eq. (1). Non-additive noise is expected to emerge in the strongly nonlinear regime close to contact and may lead to a qualitatively different spectral density [13].

This way of “listening” to an AFM may prove useful for experimenters. The second and higher harmonics in Fig. 5 (b) ($d = 0.61$ nm) should be a valuable precursor to the “snap-in” scenario that may also run the trouble of damaging the instrument. (The rumor indeed goes that experienced experimenters are capable to “listen and gauge” the good or bad shape of their instruments.)

3 Quantum and other noises

3.1 Basic noise spectra

A “noisy” signal is an erratic sequence $u(t)$ of data whose properties can only be characterized in a statistical sense. For example, the (sliding) average signal may be defined as

$$\bar{u}(t) = \frac{1}{2\tau} \int_{t-\tau}^{t+\tau} dt' u(t') \quad (4)$$

where 2τ is the averaging time. In the following, we assume that this yields a slowly varying function that can be subtracted from the data, and therefore take $\bar{u}(t) = 0$. The noise power spectral density is a measure of the fluctuations and their temporal correlations, as determined by the average Fourier transform (Wiener-Khinchine theorem [14])

$$S(f; t) = \frac{1}{2\tau} \left| \int_{t-\tau}^{t+\tau} dt' u(t') e^{2\pi i f t'} \right|^2 \quad (5)$$

If 2τ is much longer than the correlation time of the signal fluctuations, i.e., the inverse frequency width of $S(f; t)$, then the spectral density converges to a quantity independent of τ . We then get for the signal variance the Fourier representation

$$\bar{u}^2(t) = \int df S(f; t) \quad (6)$$

The quantity $[S(f; t) df]^{1/2}$ thus gives the rms signal amplitude in a bandwidth df around f . This suggests the following synthesis of a noise signal

$$u(t) = \sum_f [S(f; t) df]^{1/2} e^{i\varphi(f) - 2\pi i f t} \quad (7)$$

where f is sampled with spacing df , and $\varphi(f)$ is a randomly chosen phase (see also Ref. [10]). Alternatively, we may draw a random amplitude $A(f)$ from a complex normal distribution with variance $S(f; t) df$. To synthesize a stereo signal, real and imaginary parts of $u(t)$ may be used for the left and right channels.

3.2 Examples

The audio file [noise_thermal_quantum_white.mp3](#) (see also Fig. 6) contains three tracks of noise, computed from different spectra according to Eq. (7). The first is a classical thermal spectrum with a Drude cutoff at high frequencies, the second is quantum noise with a symmetrized spectrum, the third one is purely white:

$$\begin{aligned} S_T(f) &= \frac{kT/\tau}{1 + (f\tau)^2}, \\ S_q(f) &= \frac{hf \coth hf/(2kT)}{2\tau \sqrt{1 + (f\tau)^2}}, \\ S_w(f) &= \text{const.} \end{aligned} \quad (8)$$

We take the relatively arbitrary parameters $kT = 3hf_c$, $1/\tau = 10f_c$ and map the frequency range $0 \dots f_{\max} = 50f_c$ linearly onto the audible interval $164 \dots 8192$ Hz. The amplitudes of the spectra are normalized to a common value at ≈ 325 Hz. The main acoustic impression is that lower frequencies dominate the thermal spectrum. Quantum and white noise sound more harsh or “metallic”, and are more difficult to tell apart.¹

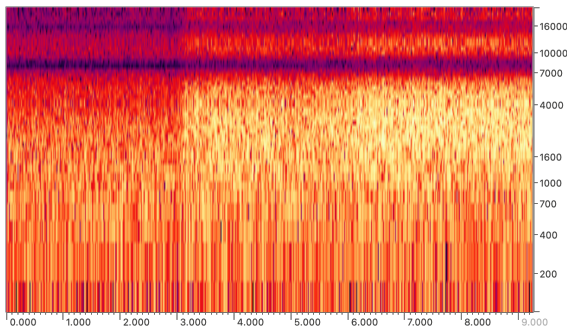


Figure 6. Synthetic noise with a thermal spectrum (first 3.25s), including quantum noise and a white spectrum (last 3.25s). The dip around 8 kHz in the spectrogram is probably due to the digital sampling.

A mixed time and frequency representation is called a spectrogram and displays as a function of time a sliding Fourier transform similar to Eq. (5) (thus providing information like a musical score). Different temporal filters

¹White noise is actually an artefact since it has infinite energy when integrated over the spectrum. The eigenfrequency spectrum of any physical system should have an upper cutoff, probably even field theories when the Planck scale is considered.

for the time window are available (rectangle, Hamming, Blackman-Nuttall etc.). Examples are given in Figs. 6, 7. The first figure displays the result of audio software analyzing the synthetic noise samples, and one sees the stronger contribution of higher frequencies, as the noise gets “quantum” or “white”. In the second example, we hear a locomotive gearing up, following nearly a diatonic scale. This “musical” signal is superimposed on broadband noise.

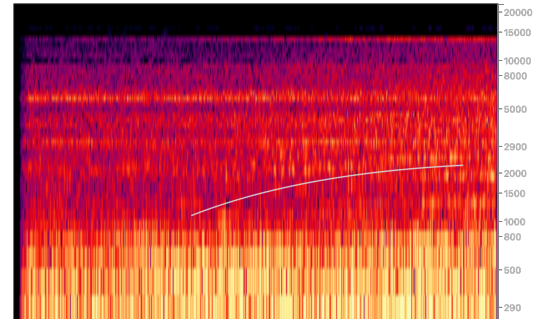


Figure 7. Spectrogram for a simple recording of a railway engine revving up. Logarithmic scale for frequency axis. A close-to-diatonic scale climbing up can be faintly seen (thin gray line to guide the eye), but is clearly discernible in the audio file [locomotive_rev_up.mp3](#). The duration shown is 4 sec.

3.3 Local energy spectrum of a Bose gas

We have discussed in a previous paper [15] inhomogeneous Bose gases and their local quantum energy density. In a typical setting, a system of a few thousand atoms is confined to a thin quasi-one-dimensional geometry, closed on one end by a potential $V(z)$. The spectrum of the energy density has been computed in the degenerate limit where most of the particles reside in the condensate mode $\phi(z)$. In the jargon of quantum field theory for the grand-canonical ensemble, this would be called the “vacuum state”. Due to interactions, however, a nonzero fraction of particles appears in excited modes denoted $v(z; f)$, even at zero temperature (“quantum fluctuations”). The frequencies f form a continuous spectrum, unless the system is closed by confinement at the other end. It has been shown that the quantum fluctuation energy in bandwidth df is given by [16, 17]

$$S(z, f) dz df = f |v(z; f)|^2 dz df \quad (9)$$

provided the $v(z; f)$ are suitably normalized (see [15]). In Fig. 8, the result of a numerical calculation is shown as a spectrogram in the zf -plane and, in a rough approximation, as a musical score. The confining potential is sketched in the upper left panel. The oscillations represent nodal lines because the modes $v(z; f)$ form standing waves at some effective potential barrier.

The sonification of these data poses the challenge of shifting the spectrum to some suitable reference frequency. Indeed, the frequency f is actually measured relative to the so-called chemical potential μ which gives the “vibration” of the condensate mode. (It is visible as the spectral weight

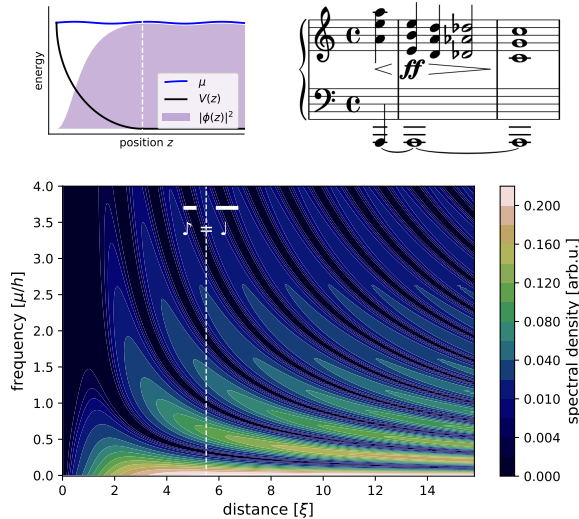


Figure 8. Local spectrum of energy fluctuations in the ground state of a Bose condensate. The system is confined to the half-space $z \geq 0$ by a “quarter-pipe” potential (top left panel). The top right panel is a crude musical score ([sonify_deep_a.mp3](#)): it tries to capture the condensate as a base tone, the lowering of the frequency spectrum and its slowing down, as one moves away from the edge position $z = 0$. Distances scaled to the healing length $\xi = \hbar/(m\mu)^{1/2}$ with the particle mass m and the chemical potential μ , typical values in Rb-87 are $\mu/\hbar = 2100$ Hz and $\xi = 230$ nm. – For the audio file [quantum_beach.mp3](#), the spectrum plotted in the lower panel is mapped into the audio range, and computed for a few positions separated by the horizontal bar lines. At the dashed line (where the potential $V(z)$ joins a flat bottom $V = 0$), the spacing is doubled (similar to a dub-step indication).

near $f = 0$ in Fig. 8, lower panel.) An oscillation at μ/\hbar is, however, not absolutely measurable because there is a phase (or U(1)) symmetry in quantum mechanics inherited from the arbitrary choice of a reference energy in classical mechanics. The situation is similar to transmitting an audio signal by frequency or amplitude modulation over the radio: the carrier frequency is irrelevant for the acoustic spectrum. We choose an algorithm similar to the noise spectra of Fig. 6 and map the range $\mu + \hbar f = \mu \dots 67 \mu/\hbar$ to the acoustic range $82 \dots 4096$ Hz, using Eq. (7) and the fast Fourier transform. The condensate which would appear with a sharply defined frequency, is not included.

The naïve musical score shown in the top right panel of Fig. 8 is based on the observation that the spectrum is dominated, at a fixed position, by a few bands with simple frequency ratios, hence the chords. This expectation is not borne out by the actual synthesized sound: it is far from musical and rather a rough reminder of aircraft noise. The frequency bands are probably too wide to allow for perceiving a collection of individual tones.

To produce a smooth “promenade” across the spatial coordinate, we have patched together noise signals of 1/3 sec each, using a mixing algorithm that weights the signal envelopes such their squared sum stays constant, as sketched in Fig. 9. This blending works well for noise sig-

nals and avoids knock artefacts from phase slips and other discontinuities.

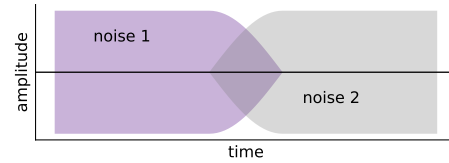


Figure 9. Mixing two noise signals while keeping constant the overall loudness impression (which is quadratic in the signal amplitude). In the overlap region of the two noise samples, the signals are multiplied with cosine and sine functions whose squares sum to unity, and then added.

4 Conclusion

A quantum physicist with some affinities to noise and music has tried himself for this paper in amateur sonification. In a few examples, I have illustrated or better: brought to the ear of the reader, how visual and audio representations are different. The two main human perceptions indeed complement themselves quite efficiently when they are confronted with a complex signal, as also observed by Iannis Xenakis:

We are capable of speaking two languages at the same time. One is addressed to the eyes, the other to the ears. The content of the communication is different but sometimes there’s a link between the two. [18]

The ear is a superb Fourier transformer and filters even weak signals out of ambient noise. A spectrum that looks clustered becomes more evenly spaced in the logarithmic scale familiar from musical notation (Fig. 4). The eye captures information at a glance, but both senses require some training and background culture to be able to identify features. The mathematical music pieces sketched here and in Ref. [3] may be fun to train your acoustic memory. An additional exercise inspired by number theory would be to use the (approximately logarithmic) distribution of prime numbers as a source of “inspired randomness” for synthesizing a sequence of notes. Finally, the examples from atomic physics have brought forward the unusual separations of time scales related to high quality factors (Sec. 2.3) – or conversely the fairly broad spectral structures in the local density of quantum energy fluctuations (Sec. 3.3).

As a final exercise, I would suggest to sonify the jump dynamics of an individual quantum state [19, 20] and encode it in a short list of pitches (its spectrum) whose intensities are proportional to the current probability amplitudes. Stereo signals can provide a way to convey quantum coherences (relative phases) [9]. This way of “listening to the quantum” will certainly not resolve the discussion around the meaning of a quantum measurement [21], but

perhaps provide a complementary challenge to the participants' senses.

Acknowledgements. The graphics in this paper have been produced with the Matplotlib and Ocenaudio software, the musical scores with Lilypond, digits of π and e were provided by Wolfram Alpha. The research of C.H. is supported by the *Deutsche Forschungsgemeinschaft* (DFG) with SFB1636, project ID 510943930, Projects No. A01 and A04. I thank Regina Hoffmann-Vogel for shared lecturing on force microscopy.

References

- [1] International Community for Auditory Display (accessed Jul 2025). <https://icad.org>
- [2] C. Henkel, Sonification_CD25, https://gitup.uni-potsdam.de/henkel/sonification_cd25/
- [3] C. Henkel, Quantum listenings – sonification of vacuum and other noises (2025), supplementary material including π/e duet scores, [arxiv:2507.08813](https://arxiv.org/abs/2507.08813)
- [4] West-Eastern Divan Orchestra, D. Barenboim (conductor), Live in Ramallah, Warner Classics (2005/2006)
- [5] M.-H. Serra, Stochastic Composition and Stochastic Timbre: GENDY3 by Iannis Xenakis, *Persp. New Music* **31**, 236–57 (1993). DOI:10.2307/833052
- [6] A. Sommerfeld, *Atombau und Spektrallinien: Wellenmechanischer Ergänzungsband* (F. Vieweg, Braunschweig 1929)
- [7] D. Lindsay Watson, Chemical Music and its Meaning, *Science News-Letter* **19**, 262–63+271 (April 1931). <https://www.jstor.org/stable/3907287>
- [8] R. Yamada, E. Piñol, S. Grandi, J. Zakrzewski, and M. Lewenstein, Towards the Intuitive Understanding of Quantum World: Sonification of Rabi Oscillations, Wigner functions, and Quantum Simulators (2023). [arxiv:2311.13313](https://arxiv.org/abs/2311.13313)
- [9] R. Christie and J. Trayford, The Sound of Decoherence (2024). [arxiv:2412.17045](https://arxiv.org/abs/2412.17045)
- [10] M. Blencowe, M. Casey, and K. Tan, Notes on Quantum Soundscapes and Music (2025). [arxiv:2504.04624](https://arxiv.org/abs/2504.04624)
- [11] NIST atomic spectra database 78 (version 5.12), edited by A. Kramida, Y. Ralchenko, J. Reader, NIST ASD Team (2024). <https://physics.nist.gov/asd>
- [12] F.J. Giessibl, Forces and frequency shifts in atomic-resolution dynamic-force microscopy, *Phys. Rev. B* **56**, 16010 (1997). DOI:10.1103/physrevb.56.16010
- [13] T.S. Biró and A. Jakovác, Power-Law Tails from Multiplicative Noise, *Phys. Rev. Lett.* **94**, 132302 (2005). DOI:10.1103/PhysRevLett.94.132302
- [14] L. Mandel, E. Wolf, *Optical coherence and quantum optics* (Cambridge University Press, 1995), chapter 2: Stochastic Processes.
- [15] C. Henkel, Quantum borderlines: Fluctuation energies in ultracold Bose gases, *Europhys. Lett.* **150**, 56001 (2025a). DOI:10.1209/0295-5075/add760
- [16] U. Al Khawaja, J.O. Andersen, N.P. Proukakis, H.T.C. Stoof, Low dimensional Bose gases, *Phys. Rev. A* **66**, 013615 (2002), erratum: *Phys. Rev. A* **66** (2002) 059902(E). DOI:10.1103/PhysRevA.66.013615
- [17] C. Mora, Y. Castin, Extension of Bogoliubov theory to quasicondensates, *Phys. Rev. A* **67**, 053615 (2003). DOI:10.1103/PhysRevA.67.053615
- [18] B.A. Varga, *Conversations with Iannis Xenakis* (Faber and Faber, London 1996).
- [19] T. Sauter, W. Neuhauser, R. Blatt, P.E. Toschek, Observation of quantum jumps, *Phys. Rev. Lett.* **57**, 1696 (1986). DOI:10.1103/PhysRevLett.57.1696
- [20] S. Stenholm, M. Wilkens, Jumps in quantum theory, *Contemp. Phys.* **38**, 257 (1997). DOI:10.1080/001075197182342
- [21] N.D. Mermin, Physics: QBism puts the scientist back into science, *Nature* **507**, 421 (2014). DOI:10.1038/507421a